Water spring: A model for bouncing drops

2003 Europhys. Lett. 62 237

(http://iopscience.iop.org/0295-5075/62/2/237)

EUROPHYSICS LETTERS 15 April 2003

Europhys. Lett., **62** (2), pp. 237–243 (2003)

Water spring: A model for bouncing drops

K. Okumura[1,2], F. Chevy[1], D. Richard[1], D. Quéré[1] and C. Clanet[3]

[1] *Laboratoire de Physique de la Matière Condensée, UMR 7125 du CNRS Collège de France - 75231 Paris Cedex 05, France*

[2] *Department of Physics, Graduate School of Humanities and Sciences Ochanomizu University - 2-1-1, Otsuka, Bunkyo-ku, Tokyo 112-8610, Japan*

[3] *Institut de Recherche sur les Phénomènes Hors Equilibre, UMR 6594 du CNRS BP 146, 13384 Marseille Cedex, France*

(received 19 November 2002; accepted in final form 19 February 2003)

PACS. 68.03.Cd – Surface tension and related phenomena.
PACS. 68.08.Bc – Wetting.
PACS. 47.85.Dh – Hydrodynamics, hydraulics, hydrostatics.

Abstract. – It has been shown that a water drop can bounce persistently, when thrown on a super-hydrophobic substrate. We present here scaling arguments which allow us to predict the maximal deformation and the contact time of the drop. This approach is completed by a model describing the flow inside the drop, and by original experimental data.

Introduction. – A *liquid ball* is a drop which remains quasi-spherical when brought into contact with a solid surface. Different examples of such objects have recently been described: let us quote *pearl drops*, which result from the extreme hydrophobicity of the solid [1–4], *liquid marbles*, achieved by texturing the surface of the liquid [5–7], and (more classically) *Leidenfrost drops*, obtained by putting a small amount of volatile liquid on a very hot plate [8]. In such cases, quick transportation of tiny amounts of liquid becomes possible without any leak, which can be of great interest in microfluidics applications. At the same time, these systems realize pure capillary "devices", and are worth being studied for their original properties.

For example, a liquid ball (with a typical diameter 1 mm) impinging onto a solid substrate bounces off, as if it were a tennis ball hitting the ground [9, 10]. The rebounds are persistent (the restitution coefficient can be very high, of the order of 0.9), and observed in a large window of impact velocity. If the velocity is too small (typically smaller than a few centimeters per second), the drop gets stuck on the substrate. If too large (above around 1 m/s), the drop endures extreme deformation during the shock, and finally breaks into several pieces. In between, a more detailed analysis of the shock itself shows that the contact time of the drop with the substrate does not depend on the impact velocity V over a large interval of velocity [11].

In this note, we discuss the maximal deformation of this sort of "water spring", and also the value of the contact time during the shock, in particular in the limit of elastic impact (small impact velocity). These predictions are compared with original experimental data.

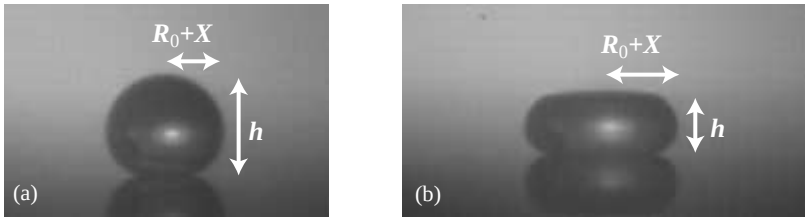

Fig. 1 – Maximal deformation of a liquid ball impinging a solid at a small velocity, (a) $R_0 \sim 0.4\,\mathrm{mm}$, $V = 0.094\,\mathrm{m/s}$, $W \sim 0.05$; or at a larger velocity, (b) $R_0 \sim 0.4\,\mathrm{mm}$, $V = 0.47\,\mathrm{m/s}$, $W \sim 1$.

We shall mainly focus on the limit of small deformations where a drop of initial radius R_0 bounces back with a high restitution coefficient of the order of 0.9. This corresponds to kinetic energies smaller than surface energies, *i.e.* to small Weber numbers, where the latter quantity is defined as

$$W = \rho R_0 V^2/\gamma. \tag{1}$$

This condition is achieved for small impact velocities, *i.e.* smaller than V_W:

$$V_W = \sqrt{\frac{\gamma}{\rho R_0}}\,. \tag{2}$$

For a millimetric water drop ($\gamma \sim 72\,\mathrm{mN/m}$, $\rho = 10^3\,\mathrm{kg/m^3}$), V_W is of the order of $1\,\mathrm{m/s}$. As seen in fig. 1, the drop at its maximal deformation looks like a flattened sphere for small impact velocities ($V < V_W$), or a pancake for larger velocities ($V \sim V_W$).

Scaling equations for a water spring ($V \ll V_W$). – We start from Euler's equation

$$\rho \frac{Dv}{Dt} = -\nabla p + \rho g, \tag{3}$$

neglecting the effect of viscosity thanks to the high restitution coefficient. We consider the limit $V \ll V_W$, in which the drop is deformed by a quantity X much smaller than the initial radius R_0 (see fig. 1a); the characteristic time of deformation scales as X/V. On the other hand, the Laplace pressure gradient scales as $\gamma X/R_0^3$ (for example, assuming an ellipsoidal form for the drop, the pressure jump at the equator or the apex scales as $\Delta p \sim \gamma/R_0(1 \pm X/R_0)$ and changes over the length R_0). Thus, eq. (3) can be dimensionally written as

$$\rho V^2 R_0^3 \sim \gamma X^2 - \rho g R_0^3 X. \tag{4}$$

This equation also expresses the transfer of kinetic energy into the surface and gravitational terms associated with the drop deformation. If the velocity is zero, the drop is deformed by gravity by a quantity δ, as first discussed by Mahadevan and Pomeau [12], which reads

$$\delta \sim R_0^3/\kappa^{-2}, \tag{5}$$

by use of the capillary length $\kappa^{-1} = \sqrt{\gamma/(\rho g)}$, which is about $3\,\mathrm{mm}$ for water.

We first consider the case where capillarity dominates gravity ($X \gg \delta$). Then, we find from eq. (4) that the maximal deformation scales as the velocity:

$$X \sim \left(\rho R_0^3/\gamma\right)^{1/2} V. \tag{6}$$

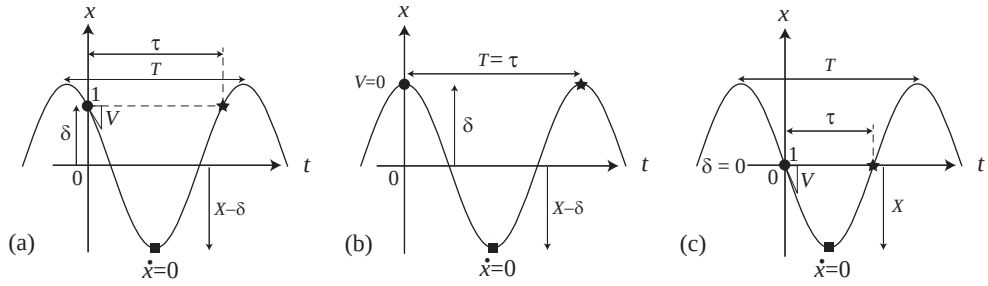

Fig. 2 – Analogy with a spring system: elongation x is plotted as a function of time t. The circle ($t = 0$) corresponds to the moment of impact and the square to the maximal deformation. The star thus indicates the moment of rebound. (a) General case. (b) Small velocity limit. (c) Large velocity limit.

The contact time should be of the order of X/V, and thus can be written as

$$\tau \sim \left(\rho R_0^3/\gamma\right)^{1/2}. \tag{7}$$

Equation (7), which yields a V-independent contact time of about one millisecond, indeed corresponds to the plateau observed experimentally [11].

Equation (6) allows us to make clear the limit of this regime. Since X must be larger than δ, we find that the velocity must be larger than a characteristic velocity,

$$V_c \sim \left(gR_0^3\kappa^2\right)^{1/2}, \tag{8}$$

which is about a few cm/s. If V approaches V_c, gravity cannot be neglected any more; we recast eq. (4) as

$$\rho V^2 R_0^3 + \gamma\delta^2 \sim \gamma(X-\delta)^2, \tag{9}$$

which expresses the energy conservation of an *imaginary* spring-mass system of initial velocity V and initial elongation δ.

Figure 2 may help to have an intuitive picture for eq. (9). The elongation x of the imaginary spring is plotted as a function of time t, setting $t = 0$ at the moment of impact. The left-hand side of eq. (9) is represented by a circle ($x = \delta$, $\dot{x} = V$ at $t = 0$), while the right-hand side by a square ($\dot{x} = 0$ at $t = \tau/2$). The moment of taking-off is marked by a star, and τ is compared in the plot with the period of the oscillator $T \sim (\rho R_0^3/\gamma)^{1/2}$.

Thus, we can graphically deduce the contact time τ. In the small velocity limit $V \ll V_c$ ($\rho V^2 R_0^3 \ll \gamma\delta^2$), we see in fig. 2b that the contact time τ is equal to the vibration period T. In contrast, in the interval commented above ($V_c \ll V \ll V_W$) and with increase in V, τ decreases from T and approaches the plateau value $T/2$. The complete variation of the contact time τ as a function of the impact velocity V will be calculated more precisely in the next section. Note finally that, as stated above, the maximal deformation, in the limit of extremely small impact velocities, tends towards the constant δ, as seen from eq. (9): we logically recover the static deformation.

Local model. – The previous scaling arguments can be completed by considering local flows during the impact. We start from the incompressibility condition ($\nabla \cdot \boldsymbol{v} = 0$), which reduces to

$$\frac{1}{r}\frac{\partial r v_r}{\partial r} + \frac{\partial v_z}{\partial z} = 0, \tag{10}$$

in the cylindrical coordinate system (r, θ, z) with $v_\theta = 0$. Looking for a solution of the type $v_r = v_r(r)$ and $v_z = v_z(z)$ satisfying appropriate boundary conditions, and introducing the equatorial radius R (see fig. 1b), we find

$$v_r = \frac{\dot{R}}{R} r, \qquad v_z = -2\frac{\dot{R}}{R} z, \tag{11}$$

setting $z = 0$ at the substrate surface. The velocity potential ϕ defined by $\boldsymbol{v} = \nabla\phi$ can thus be written as

$$\phi = \frac{\dot{R}}{R}\left(\frac{r^2}{2} - z^2\right). \tag{12}$$

If the viscosity is neglected, the dynamics of ϕ is governed by Bernoulli's equation

$$\rho\frac{\partial\phi}{\partial t} + \frac{1}{2}\rho v^2 + p + \rho g z = \text{constant}. \tag{13}$$

Here, the pressure p at the surface of the drop is given by the Laplace pressure, *i.e.* $p = \gamma C(r, z)$, where the local curvature is denoted C.

We evaluate eq. (13) at the apex ($r = 0$, $z = h$) and at the equator ($r = R$, $z \simeq h/2$), in the limit of small deformation ($\ddot{x} \gg \dot{x}^2/R_0$) for which $h \simeq 2R_0$. (Here, x is defined as in fig. 1 but not necessarily at its maximal deformation; the maximum magnitude of x is X.) To estimate the curvature difference $\Delta C = C(0, h) - C(R, h/2)$, we take the value in the static limit since we are in the regime of small velocities; the condition of constant pressure inside the drop can be integrated numerically, which gives $\Delta C = 6.8x/R_0^2$. In this way, we obtain

$$-7\rho R_0^3\ddot{x}/2 + 6.8\gamma x - \rho g R_0^3 = 0. \tag{14}$$

Writing $\delta = \kappa^2 R_0^3/6.8$ and $\omega^2 = 12.8\gamma/(7\rho R_0^3)$ (which gives as a plateau value for the contact time $T/2 = 2.3\sqrt{\rho R_0^3/\gamma}$), we find a general solution:

$$x - \delta = x_0 \cos(\omega t + \varphi). \tag{15}$$

The initial conditions lead to the relations $\cos\varphi = \delta/x_0$ and $\sin\varphi = V/(\omega x_0)$, from which we get $x_0 = \sqrt{\delta^2 + V^2/\omega^2}$ and $X = \delta + x_0$. The time of rebound τ should be given by the equation $\delta = x_0\cos(\omega\tau + \varphi)$, with $\pi \leq \omega\tau + \varphi \leq 2\pi$. Hence, we find $\omega\tau + \varphi = 2\pi - \arccos(\delta/x_0)$ with $\varphi = \arccos(\delta/x_0)$ $(0 \leq \varphi \leq \pi)$ or

$$\tau = 2\tau_c\left(1 - \frac{1}{\pi}\arccos\left(\frac{\delta}{x_0}\right)\right), \tag{16}$$

where

$$\delta/x_0 = \left(1 + (V/V_c)^2\right)^{-1/2}.$$

The analytical result, eq. (16), is plotted in fig. 3, and allows us to recover the predictions made via fig. 2: the contact time decreases by a factor 2 when the impact velocity is increased from about V_c to V_W.

Experiments. – We measured the contact time of bouncing drops at small impact velocities for millimetric water droplets hitting a super-hydrophobic substrate. Rebounds were sequentially recorded with a high-speed camera with a typical sampling time of 10^{-4} s for a contact time around 10^{-3} s, which gives a precision higher than 10%. The results are plotted in fig. 4 for two drop sizes. We indeed observed that the contact time significantly increases at

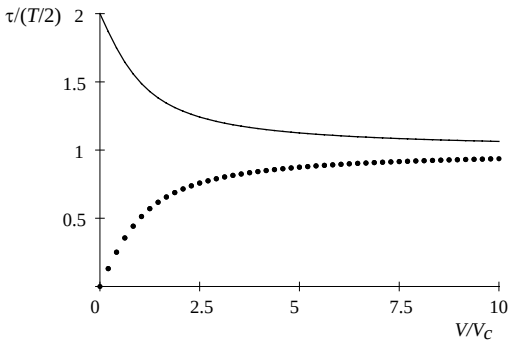

Fig. 3

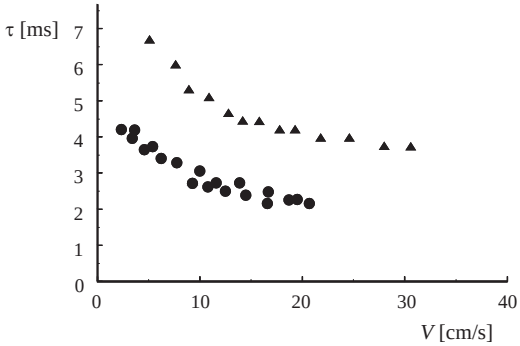

Fig. 4

Fig. 3 – Contact time τ *vs.* the impact velocity V in the elastic collision limit. The line is calculated from eq. (16). The dotted line corresponds to the case of inverted gravity (see the text).

Fig. 4 – Contact time of a water drop bouncing on a super-hydrophobic substrate as a function of impact velocity. Triangles correspond to $R_0 = 0.6 \pm 0.06\,\text{mm}$, and circles to $R_0 = 0.4 \pm 0.04\,\text{mm}$.

low impact velocity (in the range below 10 cm/s). In addition, the ratio between the largest and the shortest times is found to be very close to 2, for both sizes. Finally, the velocity above which a plateau is observed increases with the drop size.

All these observations are qualitatively in agreement with our predictions. A fully quantitative comparison would require a very accurate measurement of the drop radii (which determine the value of V_c), and also taking into account the possibility for the drop to stick at very small velocity: for $V \sim V_c$, it is observed that the drop does not bounce off but remains stuck to the solid. In contrast, the comparison between the model and the data becomes quite precise at higher speeds: the plateau value is well described by eq. (7) with a numerical coefficient of 2.6 ± 0.1 [11], in good agreement with 2.3, the value obtained above.

We also measured the maximal deformation X of the drop during the impact as a function of the impact velocity V (fig. 5). We found a linear behavior, in agreement with eq. (6).

This first series of experiments confirms that the contact time of the bouncing drop deviates from its asymptotic value when we are in the regime of low impact velocity, *i.e.* in the linear regime of deformation. We interpreted this effect as due to gravity, and tried to confirm this interpretation thanks to a second series of experiments. There, we studied the bouncing with gravity working in the opposite direction (*inverted gravity*). Drops were dropped from centimetric heights onto a super-hydrophobic substrate slightly tilted. After bouncing off, they hit at a height close to their maximum rebound height on a second plate of the same nature and inclined by the same angle. We recorded the contact time for rebounds on this second plate. The data are plotted in fig. 6, as a function of the impact velocity. The error bars are there larger (because of the experimental resolution and the effects due to the vibrations induced by the first impact), but the data clearly indicate that the contact time *increases* with the impact velocity. This is in agreement with our theory: transforming g into $-g$ (equivalently, δ into $-\delta$) in eq. (16) makes τ increase with V as plotted in the dotted line in fig. 3. Interestingly, here, the contact time can vary between 0 and τ (between τ and 2τ in the previous experiments) which can be understood qualitatively using the construction suggested in fig. 2. In the inverted gravity case, the whole sequence takes place below the line $x = 0$, so that we recover that the contact time should vary between 0 and τ.

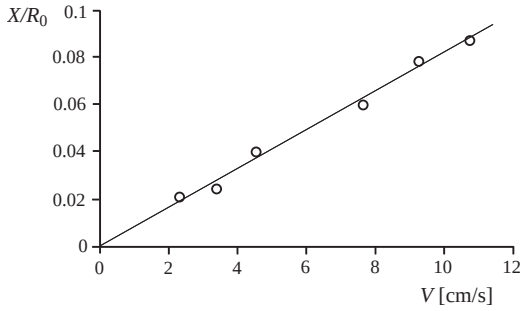

Fig. 5

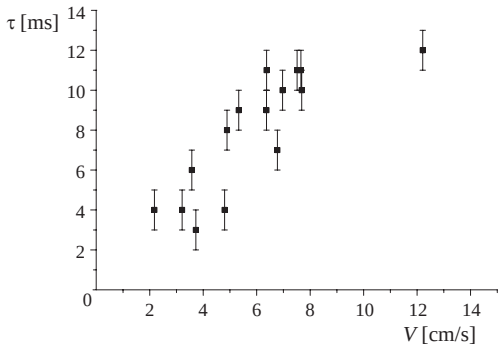

Fig. 6

Fig. 5 – Maximal deformation X of a water drop ($R_0 \sim 0.4\,\mathrm{mm}$) as a function of its impact velocity. Experimental data (circles) are compared with the scaling prediction (line) of eq. (6).

Fig. 6 – Contact time of a water drop ($R_0 \sim 1\,\mathrm{mm}$) in the field of an inverted gravity.

Perspectives. – Interesting perspectives can be given in the regime of higher impact velocities ($V > V_W$), where the drop is highly deformed and makes some kind of (transient) pancake of radius $R_0 + X \sim X$ and thickness h (fig. 1b). Since the drop crashes on the solid during a *crashing time* R_0/V, we expect the inertial term in Euler's equation to be of the order of $\rho V^2/R_0$. The Laplace pressure scales as γ/h at the equator and it changes over the length h. The pressure gradient thus scales as γ/h^2. The gravity term can be neglected in this regime of large deformation, so that Euler's equation can be cast dimensionally into

$$\rho R_0^3 V^2 \sim \gamma X^4/R_0^2 \tag{17}$$

via the conservation of the volume ($R_0^3 \sim hR^2$). Thus, the maximal size of the pancake is deduced as

$$X \sim R_0 W^{1/4}, \tag{18}$$

where W is defined in eq. (1). X is indeed found to be larger than R_0 for $W > 1$. We note that if the initial kinetic energy were transformed mainly into a surface term, namely,

$$\rho R_0^3 V^2 \sim \gamma X^2, \tag{19}$$

we would find $X \sim R_0 W^{1/2}$ instead of eq. (18).

Equation (17) is in striking contrast with the case of a small deformation where the kinetic energy was found to be stored in surface (and gravitational) energy during the shock as in eq. (4). Namely, eq. (17) tells us that the initial energy is transferred primarily into other forms, identities of which (internal flow in the pancake, and possibly, the phonon energy of the substrate, etc.) remain to be clarified.

In this regime, the contact time can be regarded as the dewetting time of the pancake. In this inertial case, the dewetting velocity V_d scales as $\sqrt{\gamma/(\rho h)}$ [4], which corresponds to the retraction speed of a liquid sheet [13]. Thus, the contact time is given by $\tau \sim X/V_\mathrm{d}$, which happens to result in eq. (7). Indeed, the contact time was observed to be independent of V and to increase as $R_0^{3/2}$ even for such high velocities [11]. This fact emphasizes that the drop is no longer in a linear-spring regime, for which eq. (19) would hold, and the contact time would be given by $\tau \sim X/V$. Note also that both X/V_d and X/V are certainly much longer than

the crashing time R_0/V in the present case ($W \gg 1$), which justifies our previous estimation of the inertial term in eq. (17).

Conclusion. – In the limit of small deformations (*i.e.* for small impact velocities), a liquid ball thrown on a solid behaves as a quasi-ideal spring. This can be understood as a conventional spring-mass system with a stiffness given by surface tension and a mass given by that of the ball; the deformation of the small ball during the impact linearly depends on the impact velocity and the contact time scales as the period of this spring-mass system, as observed with high speed photographs. The contact time was found to *increase* (typically by a factor of 2) at small impact velocity, which can be interpreted as the result of the weight of the ball. This was confirmed by achieving a similar experiment in an inverted field of gravity, which indeed leads to a *decrease* of the contact time at small velocities.

In this system, the effect of viscosity could be ignored. This might be physically due to the absence of a contact line in a situation of non-wetting; most of viscous dissipation usually takes place near the contact. It would be interesting to see how our views would be modified when the viscosity of the liquid forming the ball is increased. Extensions to similar (but different) systems such as gel balls [14] or drops of surfactant solution would also be worth studying.

* * *

We thank Y. Tanaka for useful discussions. KO is grateful to P.-G. de Gennes and to the members of his group for their warm hospitality during his second and third stays in Paris. The second stay was financially supported by Joint Research Project between JSPS and CNRS while the third by Collège de France. This work is also supported by an internal grant of Ochanomizu University.

REFERENCES

[1] Onda T., Shibuichi S., Satoh N. and Tsujii K., *Langmuir*, **12** (1996) 2125.
[2] Tadanaga K., Katata N. and Minami T., *J. Am. Ceram. Soc.*, **80** (1997) 1040.
[3] Bico J., Marzolin C. and Quéré D., *Europhys. Lett.*, **47** (1999) 220.
[4] de Gennes P.-G., Brochard-Wyart F. and Quéré D., *Gouttes, Bulles, Perles et Ondes* (Belin, Paris) 2002.
[5] Aussillous P. and Quéré D., *Nature (London)*, **411** (2001) 924.
[6] Mahadevan L., *Nature (London)*, **411** (2001) 895.
[7] Nathan P., Richard D., Foster W. and Mahadevan L., *Proc. R. Soc. London, Ser. B*, 02PB0036.1 (2002).
[8] Frohn A. and Roth R., *Dynamics of Droplets* (Springer Verlag) 2000, and references therein.
[9] Hartley G. S. and Brunskill R. T., in *Surface Phenomena in Chemistry and Biology*, edited by Danielli J. F. (Pergamon Press, London) 1958, pp. 214-223.
[10] Richard D. and Quéré D., *Europhys. Lett.*, **50** (2000) 769.
[11] Richard D., Clanet C. and Quéré D., *Nature (London)*, **417** (2002) 811.
[12] Mahadevan L. and Pomeau Y., *Phys. Fluids*, **11** (1999) 2449.
[13] Taylor G. I., *Proc. R. Soc. London, Ser. A*, **259** (1960) 1.
[14] Tanaka Y., Yamazaki Y. and Okumura K., *Bouncing gel balls* (2003), cond-mat/0302167.